Seismic response analysis of small-to-medium-span bridges considering aging plate rubber bearing

Bingzhe. ZHANG[(1)], Kehai. WANG[(2)], Guanya. LU[(1)], Wenhua. QIU[(1)]

[(1)] PhD Candidate, School of Transportation, Southeast University, 230189663@seu.edu.cn
[(2)] Professor, School of Transportation, Southeast University, kh.wang@rioh.cn

Abstract

The changes in mechanical properties of the U-SLEBs (unbonded steel-reinforced laminated elastomeric bearings) after aging affect the seismic performance of the small and medium span bridges in China. Considered the influence of rubber materials, vertical compressive stresses and loading speeds, etc., the friction behaviors, and stiffness of initial and atmospherically aged plate rubber bearings were compared by performing the horizontal cyclic loading tests of the plate rubber bearings. Based on that, the dynamic incremental analysis of a three-span pre-stressed concrete continuous girder bridge was carried out, and the influence of the mechanical properties of the plate rubber bearing before and after aging on the seismic response of the structure was compared and analyzed. The results show that the stiffness of the aged bearings becomes larger and the surface friction coefficient decreases after aging. The changes in mechanical properties of the plate rubber bearings after aging have a great influence on the internal force of the piers and pile foundations. The aging of plate rubber bearings should be taken into consideration when evaluating the seismic performance of existing bridges.

Keywords: Bridge engineering; Plate rubber bearing; Aging; Pseudo-static test; Seismic performance;

1. Introduction

SLEBs(Steel-reinforced laminated elastomeric bearings) are commonly used in small and medium-span beam bridges in China. Due to their friction and slip characteristics under earthquakes, they can effectively reduce the internal force of the pier [1]. SLEBs are made by vulcanizing and bonding a rubber material and a steel plate. Varieties of factors impact the rubber material and the adhesive layer, including ultraviolet radiation and temperature changes, and a certain degree of mechanical characteristics changes with time. From the actual bridge detection and disease investigation, it was observed that a large number of plate rubber bearings have typical aging damage such as bearing deformation, aging, position shift, emptying, and protective layer bulging under the effect of environmental meteorological conditions [2]. The aging of the performance of seat material and the change of contact surface will affect the shear stiffness, normal deformation and friction characteristics of the seat to varying degrees. Therefore, the aging of bearing will affect the dynamic response of the small-span beam bridge under earthquake.

Fig. 1 - Example of bridge damage during Wenchuan earthquake

With regard to the influence of SLEBs on the seismic performance of bridges during normal use, a large amount of research is based on the Coulomb sliding criterion. At present, scholars have conducted studies on the friction and sliding properties of bearings and mechanical properties after sliding. Wang Kehai [3-4] proposed the design concepts of "multi-channel fortification, graded energy consumption" and "one control and three easy (controllable damage site, easy detection of damage site, easy maintenance, easy replacement)" for seismic design of small-to-medium-span bridges and consideration of bearing friction and sliding. The design method of displacement allows the bearing to preferentially slip under earthquakes, but it needs to cooperate with an effective limit device. Tobias et al. [5] also pointed out that rubber bearings and connecting members with limit devices can occur preferentially destroy and dissipate some energy in earthquakes. With the increase of the service time of initial bridges, the occurrence of a large number of typical diseases and the frequent occurrence of safety accidents, researchers have gradually noted the damage performance and overall safety performance of service structures. The service life of plate rubber bearings is not less than 15 years based on Chinese domestic industry standards [6]. The numerical simulation method focuses on the analysis of shear properties, friction slip properties, and compression shear failure properties of this type of support. Compressive stress, geometric configuration, and interface contact conditions are mainly considered among them [7-9]. The friction coefficient of the bearing decreases with the increase of the positive pressure and is related to the sliding rate and the roughness of the interface. When the shear deformation of the bearing is small, only the elastic shear deformation occurs. After the bearing slides significantly, the change of effective shear deformation is small. The constitutive model of the isolated bearings considering the aging effect was calculated to define the material constant of the Moony-Rivlin model after the aging test by the least square fitting method. The study of performance and the design of full life performance of this type bridge were provided theoretical support. The change law of the properties of rubber materials in rubber bearings should be considered under the effects of aging and sea erosion. The test results show that aging is the main factor affecting the performance of rubber materials [10-12].

The small-to-medium spanning highway bridges are generally simply supported girder bridges or continuous girder bridges with a single span of no more than 40 m. The superstructure is usually supported by SLEBs, which directly contact the girders and substructures without any anchoring. With this in mind, this study presented a series of laboratory tests of the SLEBs in order to investigate their responses under cyclic loading. The responses of the aged SLEBs were compared with the initial behavioral characteristics. Effective analytical models of a three-span continuous bridge were able to simulate the realistic seismic behaviors the initial and aged SLEBs using nonlinear analysis program SAP2000. The seismic responses and damage mechanisms of the bridge were discussed. Finally, the influence of aging SLEBs should be considered when evaluating the seismic performance of existing bridges.

2. Experimental Program.

2.1 Description of the Test Specimens.

In this research study, there are seven circular laminated elastomeric with 370 mm diameters. The initial mechanical parameters of the bearings were tested in the laboratory. After four years of natural atmospheric aging, the mechanical parameters after aging were tested again. The experimental conditions, equipment and contact materials of the two experiments were consistent. Table 1 presents the specific geometric parameters and material properties. The SLEBs without thick end plates which were marked as Y1 were made up of neoprene materials. The SLEBs without thick end plates which were marked as Y2 used natural rubber. All of the specimens of both type Y1 and type Y2 were not set on thick end plates (Fig 2).In accordance with the Chinese rubber bearings test methods, the manufacturer conducted some tests on the supplied rubber to ensure that all the rubber properties met the specifications for the designs of highway bridge elastomeric bearings, as specified in the Chinese Standard [6]. The Rubber characteristics values are shown in Table 1,

Table 1 - Test specimen characteristics.

bearing type	Elastomer layer			Shim T_s (mm)	Shaper factor	Average hardness (Shore A)	Shear modulus (MPa)	Rubber material	Quantity
	t(mm)	Quantity	t_r(mm)						
Y1-initial	7	10	70	3	13.21	62	0.95	Neoprene	4
Y2-initial	7	10	70	3	13.21	64	1.01	Natural	3
Y1-aged	7	10	70	3	13.21	-	-	Neoprene	4
Y2-aged	7	10	70	3	13.21	-	-	Natural	3

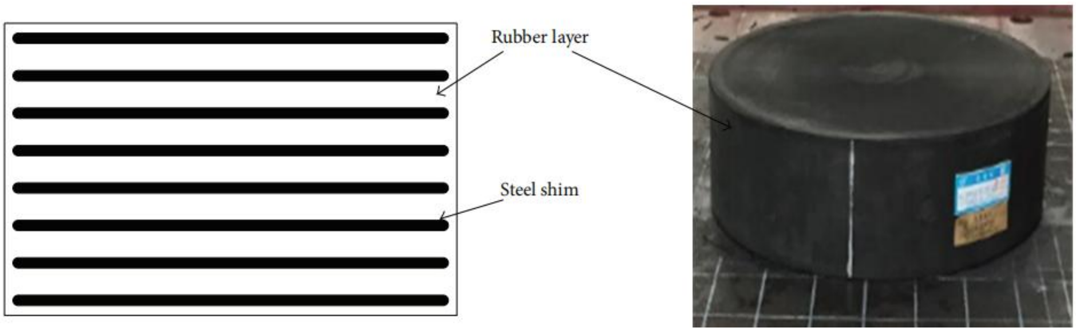

Fig. 2 - Sketch of testing specimens: bearing type Y1/Y2.

2.2 Test Setup and Procedure.

This study's testing procedures were performed in the Experimental Center at the Hengshui China Railway Construction Engineering Rubber Co., Ltd. The experimental apparatus that was used is detailed in Fig. 3 and included a seven-channel coordinated loading system with a maximum loading capacity of 30,000 kN. A typical testing bearing that was positioned between two steel plates is shown in Fig. 3. For each of the SLEB specimens, there were no restraints of the horizontal movements other than friction, and the deformation of the testing protocols included the rubber shear deformations and sliding distances. The measurement of the equivalent shear strain (ESS) was used to describe the deformation. Two steel rulers were fixed to the top and bottom supporting steel plates, respectively. A vertical white line was drawn on the side surfaces of each specimen in order to measure any possible relative deformations. A white gird measuring 10 cm × 10 cm, as well as the outlines of the specimens, was marked on the supporting surfaces of each steel plate in order to obtain more accurate measurements of the sliding ranges. Immediately after the completion of each test, a tool knife was used to erase rubber residue on the supporting surfaces of the steel plates, and the surfaces were scrubbed clean. The next test was performed after the steel plate surfaces had cooled in order to ensure the same contact friction conditions.

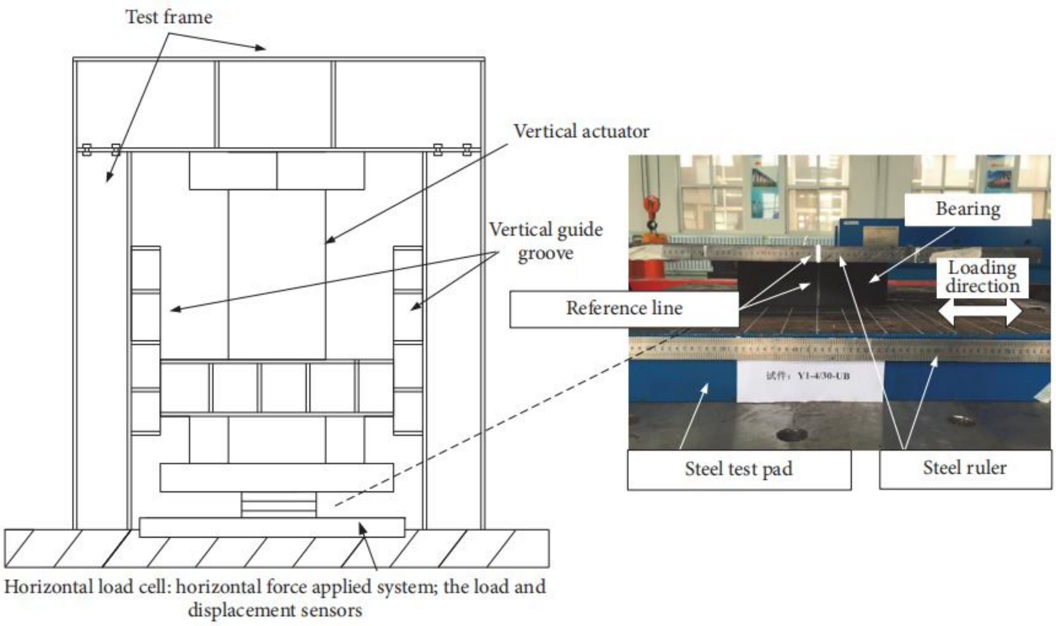

Fig. 3 - Testing setup.

The parameters for each of this study's tests are summarized in the testing matrix laid out in Table 2. First, the vertical compressive stress applied by the vertical actuators was maintained at a constant value. Then, cyclic horizontal displacement was imposed on the bottom supporting steel plates by horizontal actuators. The measurement of the equivalent shear strain (ESS), which is the ratio of the loading displacement to the thickness of the rubber layer t_r, was performed. A target of 400% ESS was determined for the testing program. The testing protocol shown in Fig. 4 was carried out in turn according to ESS, of which the levels were as follows: 25% (4) → 50% (4) → 75% (4) → 100% (4) → 150% (4) → 200% (4) → 250% (8) → 300% (8) → 350% (8) → 400% (8), where the values in brackets represent the reversed cycles per level. Each level conducted four reversed cycles when the ESS was less than 250% and increased to eight cycles after reaching 250% ESS in order to accurately analyze the bearings' performance degradation under multiple cycles of the large displacement demands.

3. Test Results and Discussion.

3.1 Responses and Horizontal Equivalent Stiffness of the Initial SLEBs and Aged SLEBs.

The laminated elastomeric bearings with initial and aged conditions exhibited significantly different responses under the same loading conditions. Due to the different aging states of the rubber layer, the force-displacement hysteresis curves and failure processes of the two sets of SLEBs are different. The main reason is the aging of the rubber material and the denaturation of the vulcanization layer connecting the steel plate layer and the rubber layer inside the bearing, which results in the plate rubber bearing. In general, compared with the initial SLEBs, the initial overall stiffness, surface friction coefficient, and stiffness of the component increase with displacement. The hysteresis curves of the initial and aged SLEBs specimen groups of Y2-8-3 are selected for further analysis, as shown in Fig. 4, where the thick solid line in the figure is the skeleton envelope.

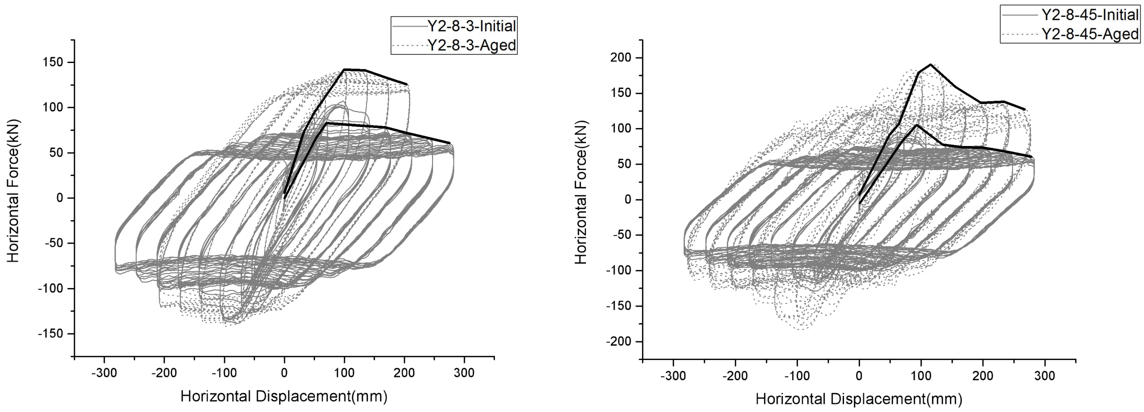

(a) (b)

Fig. 4 - Force versus displacement results for the cyclic tests: (a) Y2-8-3; (b) Y2-8-45.

During the whole test, the deformation state of the plate rubber support mainly includes: elastic shear deformation of the rubber layer-warpage of the top and bottom surfaces of the support-slip of the support-failure of the support. When the ESS is less than 75%, elastic shear deformation occurs in the rubber layer of the initial bearing, and the force-displacement relationship is basically a straight line, while the ESS of the aged bearing showing the same characteristics is 100%. When the ESS of the initial bearing exceeds 75%, the friction boundary between the bearing and the contact surface warps, resulting in a reduction in the friction area and the stiffness of the bearing begins to decrease. Increasing the curve with a negative slope, the stiffness of the bearing began to decrease significantly when the aged bearing was about 100% -125% of the ESS. When the ESS of the initial bearing reached about 100% -150%, it was observed that the friction and slip of the bearing began to occur. The equivalent horizontal stiffness value was reduced by about 20% from the figure, and the ESS of the aged bearing was about 200%. At the beginning, slippage occurs, and it can be seen from the figure that the proportion of stiffness reduction is higher than that of initial bearings. The horizontal equivalent stiffness value is reduced by about 25% -30%. The slip points of the initial and aged bearings are marked as shown in Fig. 4. As the ESS increased to 200%, a large amount of rubber debris appeared on the top and bottom contact surfaces of the initial and aged bearings. The horizontal force of the aged bearings decreased significantly, and the stiffness was decreased by 30%. After that, the horizontal displacement continued to increase, and it was found that the friction between the contact surfaces of the initial and aged bearings was basically stable, and the horizontal force was basically maintained at a certain level. In general, the initial and aged bearings can maintain a stable hysteretic relationship under large displacements. Due to the aging of the rubber material of the aged bearings, the reduction of the horizontal bearing capacity is higher than that of the initial bearings. There was no obvious failure of bearing capacity in the group of supports, and there was no tear on the surface of the supports.

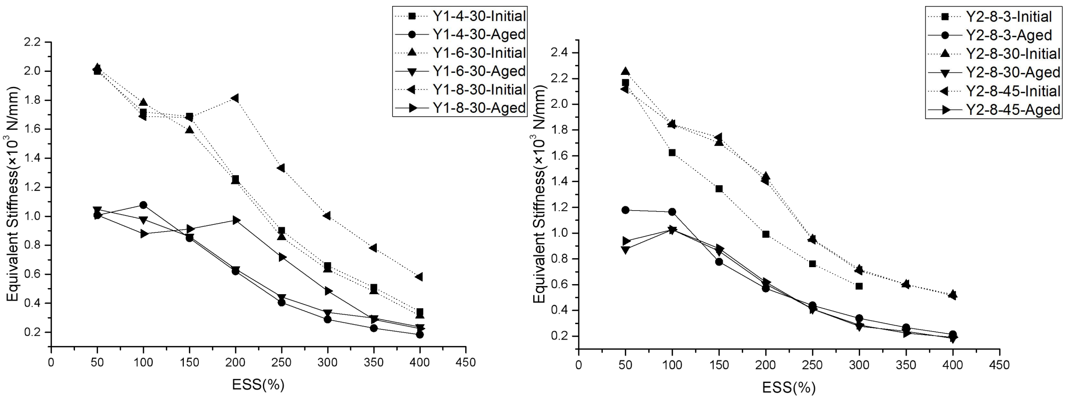

(a) (b)

Fig. 5 - Observed equivalent stiffness versus ESS: (a) Y1-Specimen; (b) Y2-Specimen.

The Fig. 5 shows the changes in the horizontal equivalent stiffness of the plate rubber bearings of the initial and aged two groups of bearings considering different influencing factors with ESS. With the increase of ESS, the horizontal equivalent stiffness of the initial and aged two sets of bearings has gradually decreased. It can be seen from the Fig. 5 that the horizontal equivalent stiffness of the aged support is greater than the horizontal equivalent of the initial support at the same displacement. The rigidity is mainly due to the aging of the rubber material and the denaturation of the vulcanization layer that connects the steel plate layer and the rubber layer inside the support, resulting in a significant increase in the overall rigidity of the plate rubber support. With slight slip, the magnitude of the decrease in the horizontal equivalent stiffness of each support is relatively small. Between 150% and 250% ESS, the bearing has obvious slippage, and the bearing is severely worn. The horizontal equivalent stiffness decreases significantly with the increase of ESS. For Y1-4 / 30-AGED, Y1-6 / 30-AGED and Y1-8 / 30-AGED, the equivalent stiffness decreased by 58.9%, 51.3%, and 44.2%, respectively. For Y1-4 / 30-INITIAL, Y1-6 / 30-INITIAL, and Y1-8 / 30-INITIAL, the equivalent stiffness decreased by 46.4%, 46.1%, and 20.8%, respectively. When the ESS exceeds 250%, the friction characteristics of the contact surface tend to stabilize, the horizontal force of the support is almost unchanged, and the decrease in the horizontal equivalent stiffness tends to be gentle. The thick solid line in Fig. 3 indicates that due to the single aging of the rubber material, the stiffness difference between the initial and aged bearings is large, and the equivalent stiffness ratio is about 1.75: 1 to 1.97: 1. When the maximum ratio is 75% ESS, the initial and aged bearing's equivalent stiffness ratio of bearing is 1.97: 1.

3.2 Friction Factor.

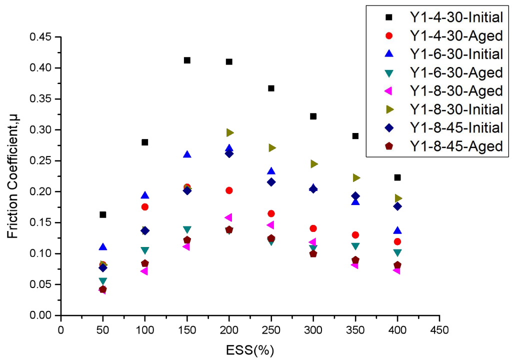

(a)

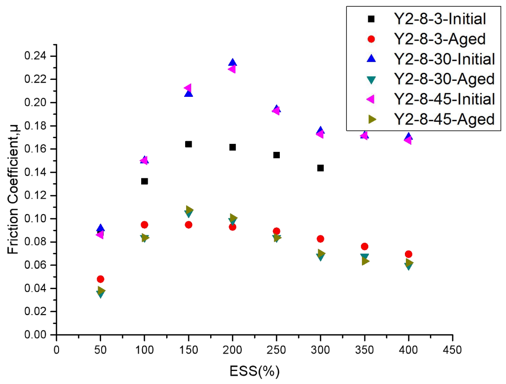

(b)

Fig. 6 - Observed friction versus increasing ESS: (a) Y1-Specimen; (b) Y2-Specimen.

Fig. 6 contains the sliding friction factors values of all bearings under each load displacement after sliding. It can be seen that the friction factor of the aged bearing is much lower than that of the surface of the initial bearing, such as the average friction factor ratio of Y1-4/30-aged and Y1-4/30-initial is 0.495:1. As the effective displacement increases, the sliding friction factor of the support first increases and then decreases. The equivalent displacement increases from 0 to 150%. At this time, the friction coefficient of the support increases linearly with the static friction between the steel plate and the contact surface. The ESS increases linearly. After more than 150%, the friction coefficient of the contact surface slowly decreases due to warpage and deformation of the bearing. Among them, the Y2-8/30-aged and Y2-8/30-initial sliding friction factors and the highest decline amplitudes are respectively 27.4% and 43.3%. Because the change of friction characteristics will affect the seismic response of the bridge, the change of friction characteristics during the sliding of rubber bearings should be considered in the seismic analysis of bridges. Fig. 6 also shows that as the loading speed increases, the friction factor will increase. As the compressive stress increases, the friction factor will decrease, and the critical sliding value of the bearing of the aged rubber material is relatively small and easier. Friction slip occurred.

3.3Mechanical Properties of Plate Rubber Bearings Considering Material Aged.

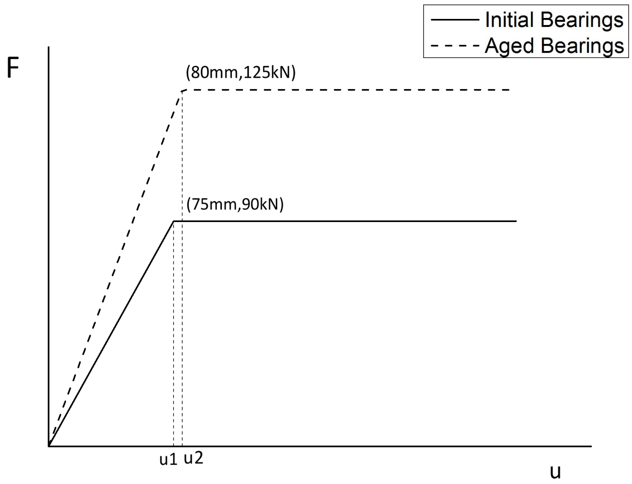

Fig. 7 - Mechanical model of SLEBs considering aged.

Existing literature often uses the double-fold line model based on the Coulomb friction criterion to consider the sliding of plate rubber bearings [5, 8], as shown in Fig. 7. Based on the test results of the plate rubber bearing, a bi-fold line model considering friction and slip damage is established for seismic analysis of the bridge, as shown in Fig. 7. Inflection point is the initial slip point of the plate rubber bearing, and its displacement value u1 is equal to the ratio of F1 to the initial stiffness; after the plate rubber bearing has suffered frictional damage, its friction and slip characteristics stable gradually. However, because the end point of interest is the process of the bearing maintaining a stable slip, a platform section is used to simplify it. According to the test results, it is recommended to take a displacement value corresponding to 400% ESS. In SAP2000, it is simulated by a double-folded line plastic connection element. In order to verify the feasibility of the model simulating friction damage of the plate rubber mount, the support test pieces Y2-8/30-initial and Y2-8/30-aged were selected respectively to verify the a. It is (75mm, 79kN), (280mm, 79kN)in the initial mount model, the inflection point and end point values of in the aged mount model are (80mm, 125kN), (280mm, 125kN).

4. Full Bridge Analysis Model Considering Bearing Aging.

4.1 Bridge Geometry and Finite Element Modeling.

In order to investigate the influences of initial and aged SLEBs as isolated bearings and discuss the damage mechanism of the small-to-medium spanning highway bridges using different SLEBs, a typical pre-stressed concrete continuous bridge, which had been constructed at the far-fault seismic action site in China, with main spans of (3 × 30 m = 90 m), was selected as a prototype for the illustration. The bridge deck was constructed with six 1.57 m high concrete box girders, and its width was 19.25 m. Type C50 concrete was used, which was obtained from Chinese code [13]. The bearings used in the bridge had the same dimensions and material properties as the type Y2 specimens. They were also produced by the Hengshui China Railway Construction Engineering Rubber Co., Ltd. It was calculated that the compressive stress of a single bearing was 8 MPa. A two-column pier was built with C30 concrete and used a circular section with a diameter of 1.4 m for the middle piers. These were reinforced with HRB 335 longitudinal bars at a reinforcement ratio of 1.02%. The diameters of the longitudinal bars used in the middle piers were 25 mm. Circular stirrups with diameters of 10 mm and a pitch of 100 mm were used for all of the piers at a stirrup ratio of 0.47%, with a concrete cover thickness of 50 mm. The calculated heights of the piers were all 12 m. The collision effect of the beam was disregard. The calculation values of the used material, along with the cross sections, were consulted using the Chinese code [14]. The bridge site belonged to type Ⅲ, and the earthquake fortification was Ⅷ [13].

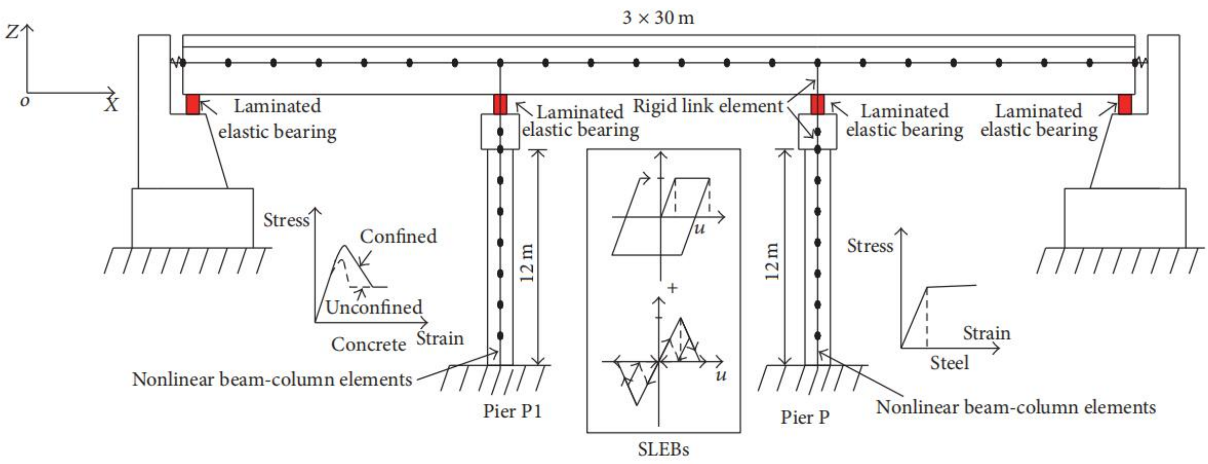

(a)

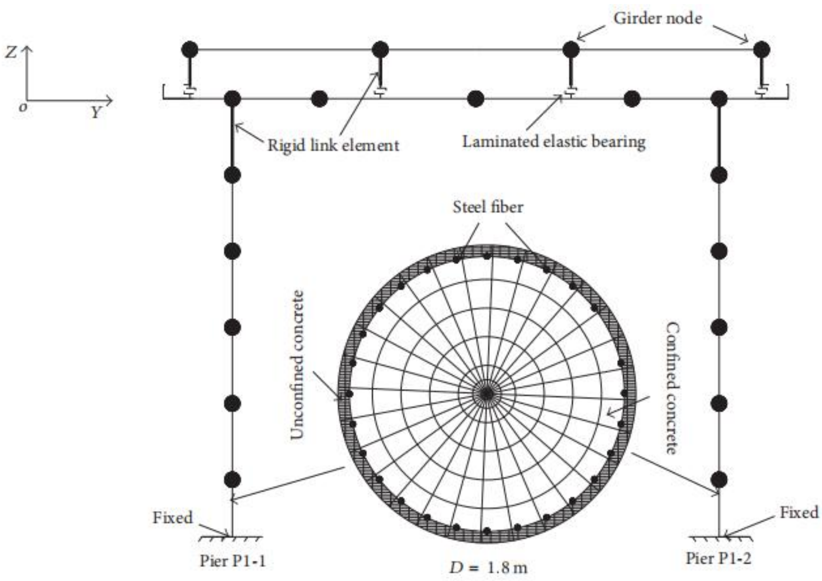

(b)

Fig. 8 - Finite element models of the prototype bridge: (a) elevation view; (b) bent elevation at pier P1.

In order to facilitate a comprehensive analytical study, a detailed nonlinear 3D finite model was developed using SAP2000 software. Since the girders and pier cap beams were not expected to be damaged under an earthquake, a linear elastic beam-column element was used. For two column piers, the seismic damage usually occurs at the top and bottom of the pier, which tends to form a plastic hinge. A nonlinear fiber beam-column element was used to model the piers. The circular section of the piers was divided into three parts consisting of confined concrete fibers, unconfined concrete fibers, and longitudinal reinforcement fibers. The column and fiber cross section properties matched within 10% of each other [15]. Using PMM fiber articulation to simulate, defining the reaming, the cross-section is divided into reinforced fibers, constrained concrete and unconstrained concrete fibers, and placed at 1/2 of the plastic hinged height. The key parameters of the shear keys could be calculated according to the realistic geometric sizes and material. The analytical models introduced in Section 3.3 were used for the laminated elastomeric bearings. The analytical model of the prototype bridge is shown in Fig. 8. Also, the pile-soil interaction was not calculated in this study.

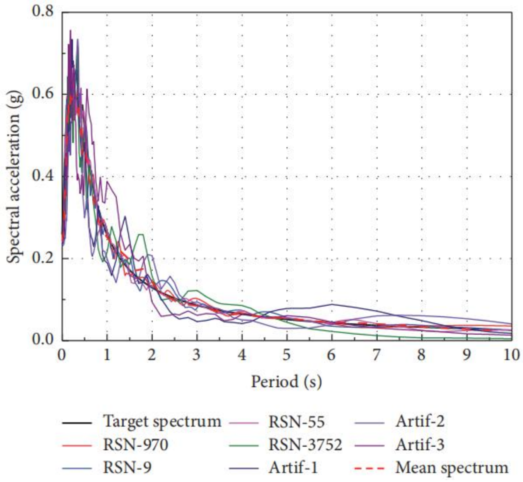

Fig. 9 - Target spectrum and the spectrum of selected ground motions.

4.2. Ground Motion Selection and Input.

First, the target spectrum was calculated according to the type of bridge site and the earthquake fortification intensity. Then, four of the actual ground motions were selected from the database of the Pacific Earthquake Engineering Research (PEER) Center, and three artificial seismic excitations were synthesized using SeismoArtif program. The response spectra of the seven ground motions, as well as the mean and target spectra, are shown in Fig. 9. It can be observed from the figure that the spectra of the analytical ground motions matched well with the target spectrum. The peak ground acceleration (PGA) values of the seven ground motions were scaled from 0.2 g to 1.0 g, at an incremental level of 0.2 g, and were input along the transverse direction. Due to the fact that the prototype bridge had been constructed at the far-fault seismic action site, the effect of the vertical seismic excitation was so small that it was neglected in this study. The average value of the calculated analytical results from the seven seismic excitations was used in this study's discussion.

5. Result Analyses and Discussion.

5.1. Seismic Responses of the Different Types of Bearings.

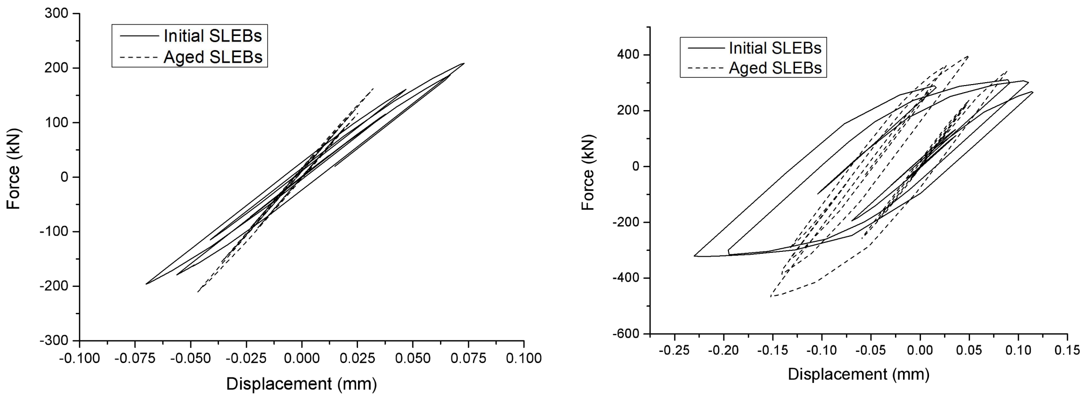

(a) (b)

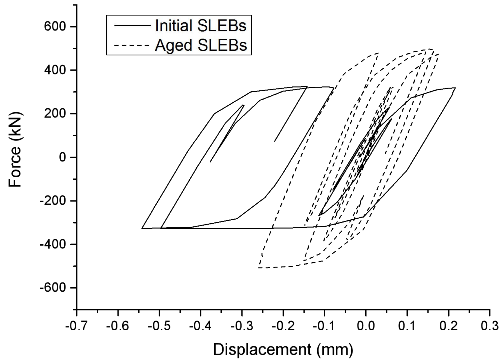

(c)

Fig. 10 - Displacement-Force of Initial/Aged laminated elastomeric bearings: (a) 0.2 g; (b) 0.6 g;(c) 1.0 g;

To illustrate the effects of frictional damage on the seismic response of plate rubber bearings, Fig. 10 lists the force-displacement hysteresis curves of the original and aging bearings under different levels of ground motion (with an actual ground motion RSN-970 Earthquake response as an example). It can be seen that the force-displacement relationship of the two bearing models maintains a linear elastic relationship before the bearing slides (peak ground acceleration of 0.2 g). Due to the bearing aging, its deformation capacity is less than that of the original rubber bearing. When the peak acceleration of the ground motion increased to 0.6 g, the original bearing significantly slipped, while the aged bearing slipped less, and the difference between the force-displacement hysteresis curves of the bearing became apparent. When the peak acceleration of ground motion was 1.0 g, both types of bearings significantly slipped. The maximum horizontal displacement of the original bearing model was 553 mm, while the aged bearing model had less slippage and the horizontal displacement was 285 mm, which was about the original. The horizontal displacement of the support is 51.5%. It shows that the rigidity of the aging bearing increases significantly, the friction and slip characteristics are weakened, and the reduction of the slip amount will greatly increase the internal force of the pier. As a result, the weakened friction and slip characteristics of the aged plate rubber bearings have a greater impact on the seismic response of the bearings.

5.2. Effects on the Damage of the Piers.

Fig. 11 shows the internal force at the bottom of P1 pier in the two bearing models under different levels of earthquakes. The average of the results of 7 ground motion analyses is taken. It can be seen that when the peak acceleration of the ground motion is 0.2 g, since the bearing has not been significantly damaged, the mechanical properties of the two bearing models are similar, which causes the seismic response of the bridge pier to be basically similar. As the peak acceleration of the ground motion increases, the internal force of the bridge pier increases with the peak acceleration. When the peak acceleration of ground motion is 0.6 g, the internal force at the bottom of the pier in the original bearing model is 8202.28 kN, while the internal force at the bottom of the pier in the aged bearing model is 9672.08 kN, and the internal force at the bottom of the pier increases by approximately 17.8%. When the peak ground acceleration reaches 0.8 g, the pier force at the bottom in the two bearing models will increase by 26.4%. When the peak ground acceleration is 1.0 g, the internal force at the bottom of the pier under the two bearing models increases by 19.3%. During the increase of the peak ground acceleration from 0.2 g to 1.0 g, the difference between the pier forces is about 20%. This shows that the aged bearing will amplify the seismic force of the pier. Although the aged bearing also has certain friction and slip characteristics, the friction energy dissipation effect of the aged bearing is much smaller than that of the original bearing. The analysis results show that the aging effect of plate rubber bearings cannot be ignored in the maintenance and maintenance of small and medium span beam bridges.

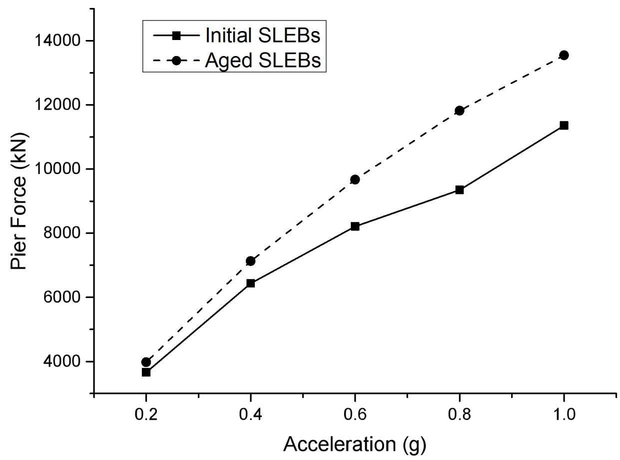

Fig. 11 - Maximum Force of pier bottom section under different level ground motions.

In this research study, based on the aforementioned discussion and the seismic damage investigation, it was found that the bridges using SLEBs displayed good seismic performances. However, the mechanical properties of aged bearings may lead to more damage to small and medium-span beam bridges under earthquakes. The bridges using SLEBs displayed good performances in controlling pier force, the bearings showed greater risks of damage, especially in the western areas with high seismicity. If the aging of the support is ignored, once the aged bearings become torn and the substructures are severely damaged, then the earthquake relief and post-disaster reconstructions will be affected. Therefore, it can be confirmed that, for small-to-medium spanning highway should be replaced the bearing in time, effective seismic isolations could be performed with low costs.

6. Conclusions

This study compared the behavioral characteristics between the initial SLEBs and aged SLEBs through a series of cyclic loading experiments. In addition, analytical models for the initial SLEBs and the aged SLEBs were proposed and compared based on the experimental results. The effects of the different types of bearings during the seismic excitations were investigated by examining the seismic responses of a typical pre-stressed concrete continuous bridge. The comparative analyses led to the following conclusions.

(1) The deformation of two types SLEBs both can be divided into three states: pure elastic shear strain of rubber layer, roll-off at the top and bottom surfaces of bearing, and obvious friction sliding. The SLEBs could potentially play the role of seismic isolation prior to unseating. The study found that the horizontal equivalent stiffness of the aged bearing is greater than the horizontal equivalent stiffness of the initial bearing at the same displacement. The overall stiffness has increased significantly. With the increase of the loading speed, the friction factor of the support will increase. As the compressive stress increases, the friction factor of the support will decrease, and the critical sliding value of the aging rubber material support will be relatively small.

(2) By comparing the bearing force-displacement curve and the pier force of the two bearing models under different levels of earthquakes, it is shown that compared with the initial bearings, the aged bearings have reduced the amount of bearing slip and the seismic force of superstructure cannot be effective dissipated by the fuse element such as bearing, the transferred pier force value increases significantly. The results show that the aging effect of plate rubber bearings cannot be ignored in the maintenance of small and medium span beam bridges.

7. References

[1] Zhuang Weilin, Chen Lesheng, etc. *Wenchuan earthquake road damage analysis - bridges and tunnels* .China People's Transport Press, 2013.

[2] Gong Yifei. Study on damage and dealing strategy of plate rubber bearing for the highway bridge. *Transportation Construction and Management*, 2014, 20: 86-90.

[3] Wang Kehai. *Bridge Seismic Research*. Version 2. Beijing: China Railway Press, 2014.

[4] WANG Kehai, WEI Han, LI Qian, et al. Philosophies on seismic design of highway bridges of small or medium spans. *China Civil Engineering Journal*, 2012, 45(9): 115-121.

[5] TOBIAS D H, ANDERSON R E, HODEL C E, et al. Overview of earthquake resisting system design and retrofit strategy for bridges in illinois. *Practice Periodical on Structural Design and Construction*, 2008, 13(3): 47-158.

[6] Laminated bearing for highway bridge (JT/T 4 - 2019), China Communication Press.

[7] Xiang Nailiang, Cui Xiaxia, Li Jianzhong. Experimental study on sliding friction behavior of laminated rubber bearing and its mechanical model. *Journal of TongJi University (Natural Science and its Mechanical Model)*, 2016, 12(44):1828-1834.

[8] Wu Gang, Wang Kehai, Li Chong et al. Parametric finite element investigation of laminated rubber bearings with friction slipping. *China Civil Engineering Journal*, 2014, 47(S1): 108-112.

[9] Buckle I, Nagarajaiah S, Ferrell K. Stability of elastomeric isolation bearings: Experimental study. *Jounal of Structural Engineering*, 2002, 1(128): 3-11.

[10] Liu Wenguang, Li Zhengrong, Zhou Fulin et al. Various dependence and duration properties of low stiffness rubber bearings. *EARTHQUAKE ENGINEERING AND ENGINEERING VIBRATION*, 2002, 22(6): 115-122.

[11] LI Yanmin, MA Yuhong, LUO Jiarun et al. The effect of aging on the material constant of the rubber isolator's constitutive model Moony-Rivlin . *EARTHQUAKE ENGINEERING AND ENGINEERING VIBRATION*, 2016, 35(16): 164-170.

[12] MA Yuhong, ZHAO Guifeng, LUO Jiarun et al. Experimental research on property deterioration of rubber material used as natural rubber isolator for offshore bridges under aging and marine corrosion. *JOURNAL OF VIBRATION AND SHOCK*, 2016, 35(6): 114-124.

[13] MOTC, JTG/T, China Ministry of Transportation and Communications Press, Beijing, China, 2008 (in Chinese).

[14] MOTC, China transportation standard: code for design of highway reinforced concrete and pre-stressed concrete bridges and culverts (JTG D62-2004), China Ministry of Transportation and Communications Press, Beijing, China, 2004.

[15] A. Aviram, K. R. Mackie, and B. Stojadinovic, "Guidelines for nonlinear analysis of bridge structures in California," *Technical Report PEER 2008*., Pacific Earthquake Engineering Research Center, University of California, Berkeley, Calif, USA.

